Aust. J. Phys., 1989, **42**, 439–50

Lunisolar Atmospheric Tides. II*

R. Brahde

Institute of Theoretical Astrophysics, University of Oslo,
P.O. Box 1029, Blindern, 0315 Oslo 3, Norway.

Abstract

In an earlier paper (Brahde 1988) it was shown that series of measurements of the atmospheric pressure in Oslo contained information about a one-day oscillation with mean amplitude 0·17 mb. The data consisted of measurements every second hour during the years 1957–67, 1969 and 1977. In the present paper the intervening years plus 1978 and 1979 have been included, increasing the basis from 13 to 23 years. In addition the phase shift occurring when the Moon crosses the celestial equator has been defined precisely, thus making it possible to include all the data. The one-day dynamic oscillation with mean amplitude 0·17 mb has been confirmed, and in addition its first harmonic or the half-day oscillation has also been found. Its mean amplitude becomes 0·048 mb, a value which is considerably higher than the amplitude 0·007 mb determined by means of data from Oslo by Haurwitz and Cowley (1969). It is also shown how the dynamic wave reacts on the thermal wave.

1. The Data

As explained in Brahde (1988; referred hereafter as Part I), data for the years 1968 and 1970–76 had been excluded because the two first digits were not always recorded. Now this has been corrected by the introduction of two tests. The data which were recorded in units of 0·1 mb (0·1 mb ≡ 10 Pa) were tested if the number was smaller than 500, or if it was greater than 500 and smaller than 1000. In the first case 10000 was added, in the second 9000 was added, thus confining the data to the interval between 950 and 1050 mb. It was also necessary to examine the data for errors. The absolute value of the difference between two subsequent pressure data points was formed and compared with a prescribed limit. Choosing the limit 9 mb it was easy to detect errors of the order of 1000, 100 and 10 mb. Inspection of the previous and the following values could also reveal errors of smaller magnitude. If one or two values were found to fall outside of an otherwise smooth series, and a correction involving addition or subtraction of an integral number of millibars caused the value(s) to fall in line, then this correction was applied. The last digit could of course never be changed.

The expanded dataset comprising the 23 years 1957–79 form a continuous series of 100 800 measured values.

* Part I, *Aust. J. Phys.*, 1988, **41**, 807–31.

0004-9506/89/040439$03.00

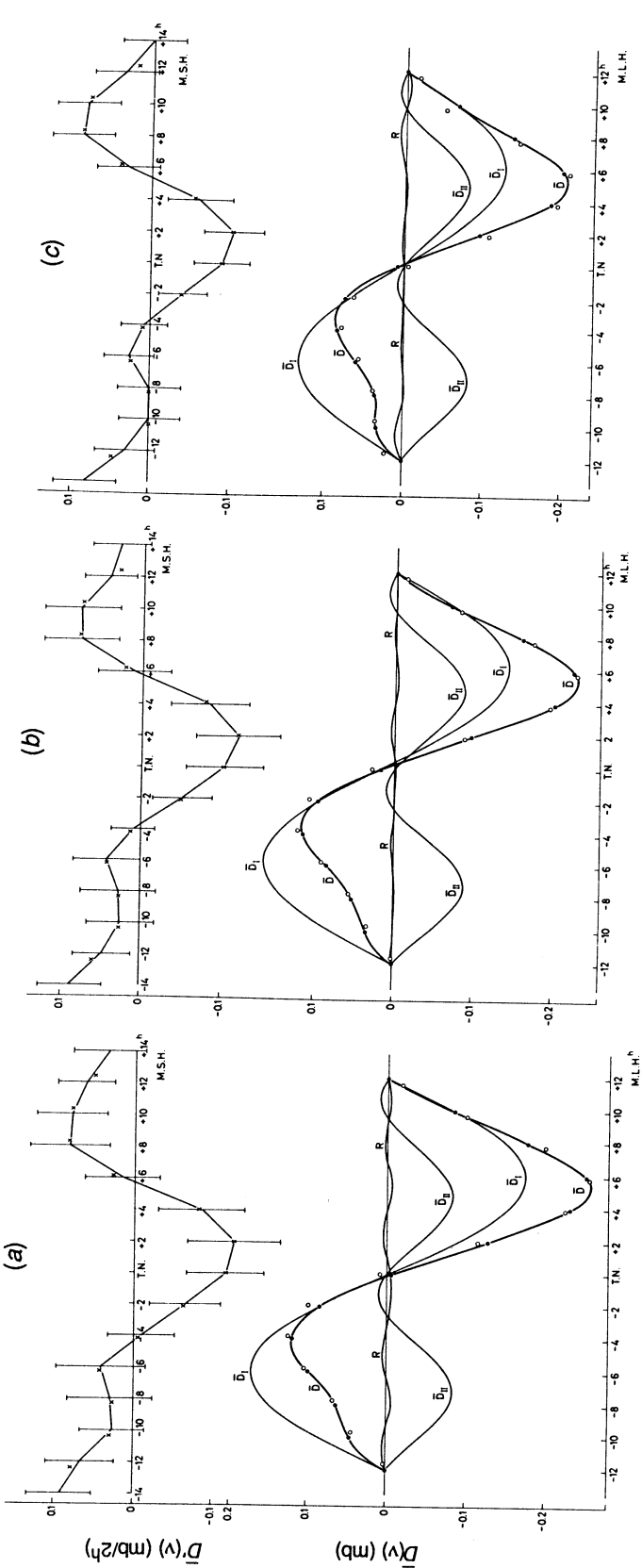

Fig. 1. Mean pressure gradient and mean dynamic pressure for (*a*) $\sigma = 0 \cdot 2$ mb ($N = 1882 = 23\%$), (*b*) $\sigma = 0 \cdot 4$ mb ($N = 3842 = 48\%$) and (*c*) $\sigma = 1 \cdot 4$ mb ($N = 7751 = 95\%$). *Upper graph*: Mean pressure gradient $\bar{D}'(\nu)$ as a function of tidal phase, measured in mean solar hours around tidal noon T.N. Crosses mark interpolated values measured in mean lunar hours around T.N. *Lower graph*: Variation of mean dynamic pressure $\bar{D}(\nu)$ with mean lunar hours around T.N., showing its harmonic components $\bar{D}_{\mathrm{I}}$ and $\bar{D}_{\mathrm{II}}$, and the sum of higher harmonics *R*. Small circles close to $\bar{D}$ represent mean values of the integrated series $D(t)$.

2. Refinement of the Method

In Part I it was shown that the principal and secondary maxima of the tidal acceleration change position relative to upper or lower culmination of the Moon, every time the Moon crosses the equator. To correct for this some days, when the time interval between maxima became shorter than 16 hours, were excluded from the statistics.

This test has now been replaced by a precise definition of the time when the Moon crosses the equator and a subsequent switch between principal and secondary maxima. (The Sun does not matter in this connection because during the two periods when it also crosses the equator, the pull of the Moon always dominates.) Consequently, all of the 8154 tidal days can be used in the statistics and the first harmonic, or the half-day oscillation, can also be studied.

With these alterations the gradient of the pressure was found and grouped within the tidal days as described in Part I. The noise limitation σ was chosen to be 0·2, 0·4 and 1·4 mb as before, and the results are shown in the upper part of Fig. 1 where the noise limit increases from left to right. Compared with Figs 4*a* and 6 of Part I we notice a maximum of the gradient at T.N.–6^h which could not be seen before.

The values of the mean gradient $\overline{D}'(\nu)$ were determined at T.N.–14^h to T.N.+14^h, where h is the mean solar hour. The integration of $\overline{D}'(\nu)$ to find $\overline{D}(\nu)$ is performed by the method described in Part I (pp. 818–19). But, since we want to separate the harmonic components of the integrated function, we should not use intervals of mean solar time around T.N. The length of a tidal day is a variable quantity, but examination of the file gives a mean value of 1·0244 mean solar days. This is sufficiently close to the length of a mean lunar day of 1^d·03505 to allow for the use of mean lunar hours in this connection. The procedure was as follows: First the coefficients of a Fourier series based on the 15 values of the gradient were determined. The resulting Fourier series was used to interpolate values in distances of −12, −10, ... +12 mean lunar hours from T.N. Crosses in the upper part of Fig. 1 mark these points. Next, these 13 points were used to compute a new set of Fourier coefficients, which in turn were used to integrate the function using formula (7) of Part I.

The results are presented in the lower part of Fig. 1 by the curves marked $\overline{D}$. The same formula allows interpolation between the 13 points which are marked by dots, thus giving a smooth shape to the curves for $\overline{D}(\nu)$. Formula (7) of Part I allows also a separation of the Fourier components of the function $\overline{D}(\nu)$, and we get the one-day and half-day components marked $\overline{D}_I$ and $\overline{D}_{II}$ in Fig. 1. The use of intervals of length 1·0244 mean solar days around T.N. did not diminish the higher harmonics, and therefore mean lunar hours were preferrred. The curves marked R show the sum of the harmonics of order 3, 4, 5 and 6.

Earlier the integration was also performed by means of another method. Based on the computation with noise limit σ = 0·4 mb, the regression coefficient between the gradient of the pressure and the magnitude* of the

* The 'magnitude' was defined to be the difference between the maximum value of the acceleration which takes place at tidal noon and its subsequent minimum value.

tidal acceleration was extracted (see Part I, pp. 808, 815) and used to compute the series $D(t)$ running through the intervals where the one-day oscillation had been determined. Now the gaps between the intervals have disappeared and the series $D(t)$ has been found throughout the 23 years every second hour, this time with the three actual values of σ. Again, as in Part I, mean values grouped within tidal phase were formed, and the results are shown in the lower part of Fig. 1 by small circles, which closely follow the curves for $\overline{D}(v)$. This of course, represents a control of the procedures and a confirmation of the correlation between tidal acceleration and the pressure variation. The first method does not involve the magnitude of the acceleration at all, and depends only on the pressure data grouped according to tidal phase. The second method depends also on the magnitude of the acceleration and its correlation with the measured pressure gradient.

Table 1. Dynamic atmospheric (luni-solar) tide

Noise limit σ (mb)	Number	(%)	Amplitude of oscillation 'One-day' A_I (mb)	'Half-day' A_{II} (mb)
0·20	1882	23	0·172±0·053	0·046±0·021
0·40	3892	48	0·154±0·059	0·048±0·018
1·40	7751	95	0·129±0·039	0·044±0·014

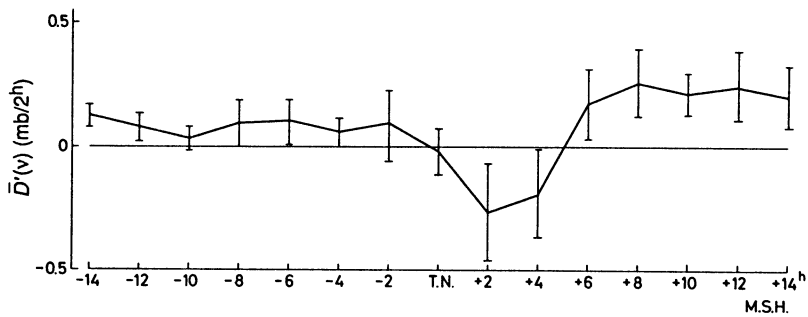

Fig. 2. Mean dynamic gradient $\overline{D}'(v)$ when the limitation of data because of noise is avoided. (Note that the scale of the ordinate differs from Fig. 1.)

As already stated the three parts of Fig. 1 differ only in the choice of noise limit σ. When $\sigma = 0 \cdot 2$ mb each point of the gradient curve represents 1882 data points or 23% of the total. With $\sigma = 0 \cdot 4$ mb the basis is 3842 data points or 48%, and for the limit $\sigma = 1 \cdot 4$ mb as much as 7751 observed values are behind each point of the curve, or 95% of the available 8154 tidal days. Table 1 summarises these values. The uncertainty in the amplitudes A_I and A_{II} have been found in the usual way by selecting data for each year separately, determining the amplitudes, forming the grand mean and computing standard deviations. Examination of the table reveals the following:

(1) the amplitude A_I in the first line coincides with the value in Part I and diminishes with increasing values of σ;

(2) the amplitude A_{II} of 0·048 mb is about seven times larger than the value 0·007 mb found by Haurwitz and Cowley (1969) for the same station; and
(3) it is surprising that the three results differ so little considering that 95% of the data was used in the third line.

Item (3) lead to a rerun of the program without the noise test, or actually the limit was set to 100 mb, which served the same purpose. In Fig. 2 the function $\overline{D}'(v)$ is shown in this case when all data were included. The variation becomes about 2·5 times larger than before, and the error bars show that the result is scarcely significant. However, it is highly interesting that the remaining 5% of the data makes such a profound difference.

Table 2. Spectrum of dynamic variation 2A

Year	$2A = D_{max} - D_{min}$ (mb)							
	0·05	0·15	0·25	0·35	0·45	0·55	0·65	0·75
1957	26	36	26	108	118	35	6	0
1958	25	40	58	110	89	31	0	0
1959	37	32	51	84	136	14	0	0
1960	23	24	61	102	103	42	0	0
1961	24	28	58	99	97	42	7	0
1962	28	31	60	79	101	56	1	0
1963	24	17	55	77	123	59	0	0
1964	24	16	56	66	117	65	12	0
1965	8	23	61	78	110	42	34	0
1966	13	30	52	71	84	59	43	1
1967	24	18	38	65	75	98	36	0
1968	32	18	25	67	63	115	37	0
1969	12	31	30	76	91	71	33	11
1970	13	36	34	73	84	63	46	4
1971	19	22	33	63	101	78	36	0
1972	28	23	29	65	90	122	0	0
1973	18	41	32	86	104	52	21	0
1974	16	43	33	104	96	51	11	0
1975	21	30	39	103	105	58	0	0
1976	31	19	48	108	129	22	0	0
1977	38	46	40	97	103	27	0	0
1978	23	44	43	108	93	36	5	0
1979	22	22	67	112	87	44	0	0
Sum	529	670	1029	2001	2299	1282	328	16

From the series $D(t)$ with $\sigma = 0·4$ mb running through 23 years we have formed a spectrum of differences between subsequent maxima and minima. Table 2 gives the results for the individual years, and the complete amplitude spectrum is presented in Fig. 3; it may be compared with the right-hand side of Fig. 8 in Part I. Table 2 reveals an interesting feature. The largest amplitudes occur around 1968, a year when the Moon attained its highest numerical value of declination, ±28°·5. As a consequence of the formation of the series $D(t)$ by means of the regression coefficient and the computed magnitude of the

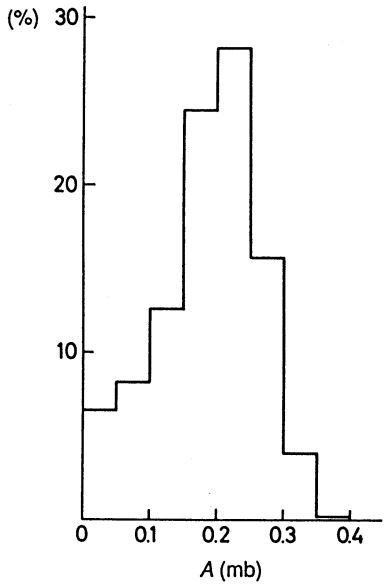

Fig. 3. Amplitude spectrum of the dynamic oscillation $D(t)$.

accleration, the amplitude is expected to be high in 1968. A high value of declination means a low value of zenith distance z, and since the principal variation of the tidal acceleration is proportional to $\cos^2 z$ this means a large amplitude. Therefore, the influence of the tide will be most conspicuous during years when the ascending node of the lunar orbit is near the vernal equinox. This happens every 18–19 years (18·613).

Looking again at the curves for the mean gradient in Fig. 1, the error bars may seem comparatively large. Because only one 18–19 year period is included, part of the uncertainty may be caused by a systematic variation within the period. A longer dataset including several periods would give an answer to this question.

The amplitude spectrum shown in Fig. 3 reveals a distribution containing more of the smaller amplitudes than in the corresponding Fig. 8 of Part I. This is because oscillations with smaller amplitudes when the Moon crosses the equator have been included with the refined method. It will be noted that the maximum now occurs at an amplitude 0·225 mb instead of 0·175 mb in Fig. 8 earlier. The mean value, however, is unaltered at 0·19 mb.

3. Evaluation of the Method

In Part I it was explained why the one-day oscillation could not be found with a method which does not include a correction every time the Moon crosses the celestial equator. However, this should not invalidate a search for the half-day oscillation. Therefore, an explanation is needed as to why the Chapman–Miller method used in earlier investigations has failed (Malin and Chapman 1970). In the first place, the use of mean lunar time introduces an error regarding the selection of data. Analogous to the 'equation of time' which is the difference between true and mean solar time, there is a varying difference between true and mean lunar time of more than twice the effect as

regards the Sun. A simple calculation of the two terms the 'reduction to the equator' and the 'equation of the centre' shows that the range of distribution becomes approximately one hour. In addition, perturbations of the Moon by the Sun add to the amount. Therefore, the use of true instead of mean lunar time would be an improvement, but this is not used in the Chapman–Miller method (see Chapman and Lindzen 1970, p. 71).

However, this would not be sufficient because of the contribution of the Sun to the tidal acceleration. Ordinarily the pull of the Moon is more than twice that of the Sun, but it is easy to find situations where the two must be about the same magnitude (see Part I, pp. 808–9). Actually the maximum acceleration occurs when a vector pointing to a position between the Moon and the Sun culminates. This is exactly the method used here. In Part I it was shown how the added vertical components of the tidal acceleration of Moon and Sun are used to produce the curve shown there in Fig. 2. The moments of tidal noon are defined to be when the curve exhibits the principal minima, representing the maxima of the acceleration.

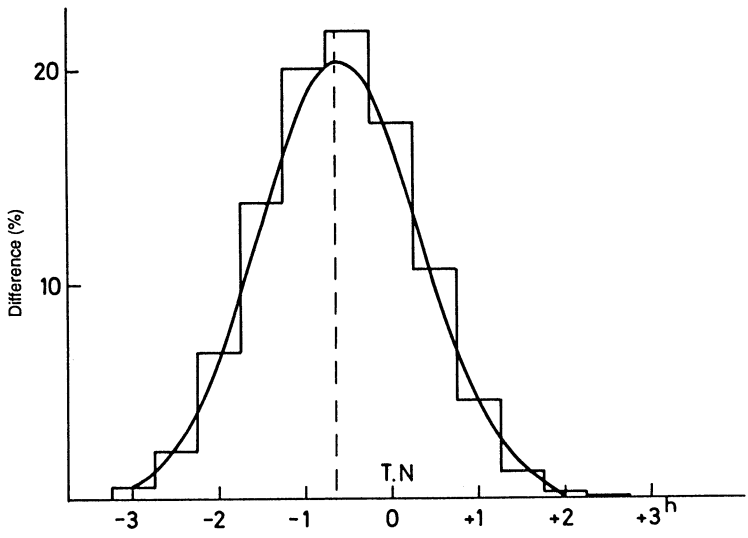

Fig. 4. Spectrum of the differences between moments of tidal noon T.N. and a running scale of length one mean lunar day.

In order to demonstrate the difference in time measure between tidal noon and mean lunar noon, a series of T.N. values running from 1 January 1957 to 31 December 1979 were compared with a measuring rod of length one mean lunar day of 1·0350502 mean solar days. The differences were recorded and care was taken to adjust for the phase shifts when the Moon crosses the equator by insertion of a half mean lunar day. The result is shown in Fig. 4. The range of the distribution has now become 5 hours, and the displacement of the axis of symmetry is caused by the arbitrary starting moment of lunar time, at lower culmination of the Moon on 1 January 1957.

Fig. 4 is a striking demonstration of the magnitude of errors which may be caused by the use of mean lunar time. It must obviously distort the expected results. Secondly, our method is aimed at the gradient of the pressure, not directly on the pressure itself which varies primarily with the weather. Thirdly, the rejection of data because of too much noise is different in the two methods. Our noise limit as defined in Part I, p. 811 was chosen as the standard deviation of 25 measured pressure values from an interpolation formula where periods shorter than $6^h \cdot 25$ had been omitted. As we have seen, this noise criterion allows 95% of the data to be used in the statistics. Conversely, Chapman in his determination of L_2 from Greenwich data (Chapman and Lindzen 1970, p. 75), selected only days on which the range during one day did not exceed 0·1 inch or 3·4 mb, and this reduced his useable data to about one-third of the total.

4. Thermal and Dynamic Terms

Since the dataset was enlarged the thermal effects were also studied again. In Part I the mean pressure gradient $\overline{T}'(\nu)$ was found from the data during 13 years when a period of 24 mean solar hours was used, incidentally with the noise limit $\sigma = 0 \cdot 4$ mb. The same procedure was repeated with the dataset of 23 years, and the running oscillation $T(t)$ was found as before.

Table 3. Multicorrelation coefficients

H	C_{FT}	C_{ST}	C_{FD}	C_{SD}	ν
−14	0·0977	−1·1634	−0·0662	−0·0036	1
−12	0·1114	−1·1861	0·0145	−0·0270	2
−10	0·0041	−1·1628	0·0618	−0·0233	3
−8	−0·0607	−1·1340	0·0905	−0·0074	4
−6	−0·0599	−1·1204	0·1222	0·0198	5
−4	0·0260	−1·1283	0·1422	0·0188	6
−2	0·1008	−1·1487	0·1165	0·0048	7
0	0·0965	−1·1551	0·0351	−0·0042	8
2	0·0086	−1·1166	−0·0817	−0·0048	9
4	−0·1151	−1·0508	−0·1884	0·0028	10
6	−0·1569	−1·0323	−0·2237	−0·0018	11
8	−0·0447	−1·0893	−0·1704	−0·0199	12
10	0·0973	−1·1653	−0·0789	−0·0347	13
12	0·1122	−1·1864	−0·0009	−0·0275	14
14	0·0055	−1·1623	0·0375	0·0054	15

In Part I we also found multicorrelation factors connecting four quantities: F, the magnitude of the tidal acceleration; S_f, the filtered daily variation of the radiative balance; T_f, the filtered daily thermal series; and D, the dynamic series. The resulting factors were given in Table 2 of Part I. With the larger dataset and the precise definition of the phase shift, the new results are given here in Table 3.

The 'corrected' series $T_c(t)$ and $D_c(t)$ are given by

$$T_c = C_{FT} F + C_{ST} S_f, \qquad D_c = C_{FD} F + C_{SD} S_f.$$

Comparison of the two tables shows that the numerical value of the factor C_{FT} has become smaller. The factor C_{ST} connecting T_c and the filtered radiation

Table 4. Statistical tests

Data: $O(t)$ are the observed pressure values; $T(t)$ and $D(t)$ the thermal and dynamic pressure variations respectively; and $R(\frac{1}{2})$ and $R(1)$ are random numbers confined to the interval $\pm\frac{1}{2}$ and ± 1 mb respectively

T.N.+	Dynamic pressure gradient $\overline{D}'(\nu)$			CET	Mean pressure gradient $\overline{T}'(\nu)$ [$O(t)$ data]			ν
	$O(t)-D(t)$	$O(t)-T(t)$	$1013+R(\frac{1}{2})$		$O(t)-T(t)$	$O(t)-[T(t)-D(t)]$	$1013+R(1)$	
−14	0·023±0·042	0·008±0·033	0·007±0·011	−2	−0·006±0·052	0·013±0·050	0·007±0·048	1
−12	0·013±0·037	0·008±0·033	−0·006±0·016	0	−0·009±0·058	−0·006±0·056	−0·004±0·034	2
−10	0·006±0·044	0·004±0·044	−0·005±0·011	2	−0·003±0·047	−0·012±0·046	0·005±0·040	3
−8	0·003±0·048	−0·008±0·047	0·004±0·013	4	−0·024±0·030	−0·027±0·029	−0·006±0·035	4
−6	0·009±0·042	−0·003±0·040	0·000±0·012	6	0·010±0·033	0·017±0·036	−0·014±0·024	5
−4	0·001±0·026	0·004±0·026	−0·000±0·013	8	0·032±0·037	0·043±0·039	0·011±0·042	6
−2	0·001±0·037	0·008±0·037	0·006±0·015	10	0·004±0·041	0·005±0·040	0·015±0·035	7
0	0·003±0·052	0·008±0·048	−0·002±0·014	12	−0·008±0·063	−0·027±0·062	0·004±0·026	8
2	0·001±0·055	0·001±0·047	−0·006±0·014	14	0·001±0·051	−0·025±0·049	−0·002±0·028	9
4	−0·004±0·048	−0·007±0·041	0·002±0·012	16	−0·006±0·042	−0·020±0·041	−0·021±0·023	10
6	0·005±0·046	0·002±0·042	−0·001±0·013	18	0·011±0·048	0·017±0·048	−0·012±0·031	11
8	0·000±0·050	0·003±0·043	0·000±0·011	20	0·019±0·032	0·042±0·033	0·020±0·031	12
10	−0·003±0·048	0·003±0·040	0·009±0·013	22	−0·005±0·052	0·014±0·051	0·008±0·048	13
12	−0·007±0·034	0·001±0·032	−0·001±0·014	24	−0·009±0·059	−0·005±0·057	−0·004±0·034	14
14	0·007±0·036	0·007±0·038	−0·008±0·016	26	−0·003±0·048	−0·012±0·047	0·005±0·040	15

Table 5. Monthly means of the series (*a*) *T*(*t*) and (*b*) *T*(*t*)–*D*(*t*)

CET	Jan.	Feb.	Mar.	Apr.	May	June	July	Aug.	Sep.	Oct.	Nov.	Dec.
						(*a*) *T*(*t*)						
0	0·233	0·386	0·188	0·120	0·155	0·109	0·005	0·022	0·034	0·025	0·148	0·135
2	0·113	0·249	0·144	0·131	0·223	0·204	0·084	0·070	0·024	−0·058	0·056	0·038
4	−0·063	0·013	−0·008	0·083	0·279	0·284	0·140	0·087	−0·036	−0·204	−0·106	−0·110
6	−0·201	−0·101	0·015	0·188	0·440	0·455	0·297	0·217	0·037	−0·207	−0·171	−0·252
8	−0·093	0·039	0·278	0·415	0·600	0·604	0·460	0·426	0·295	0·053	0·021	−0·143
10	0·160	0·257	0·433	0·442	0·512	0·526	0·428	0·461	0·437	0·291	0·239	0·104
12	0·162	0·225	0·268	0·215	0·186	0·206	0·183	0·238	0·268	0·213	0·155	0·082
14	−0·072	−0·099	−0·145	−0·150	−0·214	−0·197	−0·130	−0·109	−0·094	−0·074	−0·118	−0·116
16	−0·187	−0·373	−0·519	−0·535	−0·609	−0·572	−0·425	−0·442	−0·422	−0·245	−0·234	−0·139
18	−0·125	−0·354	−0·509	−0·615	−0·789	−0·781	−0·575	−0·561	−0·447	−0·132	−0·131	−0·002
20	−0·009	−0·178	−0·195	−0·314	−0·580	−0·623	−0·416	−0·360	−0·175	0·104	0·027	0·148
22	0·082	−0·064	0·051	0·020	−0·200	−0·214	−0·052	−0·049	0·080	0·232	0·114	0·254
						(*b*) *T*(*t*) − *D*(*t*)						
0	0·214	0·419	0·259	0·196	0·208	0·123	−0·016	−0·029	−0·044	−0·066	0·058	0·068
2	0·190	0·343	0·227	0·176	0·221	0·160	0·016	−0·009	−0·055	−0·115	0·037	0·070
4	0·087	0·140	0·066	0·092	0·231	0·198	0·040	−0·007	−0·098	−0·207	−0·039	0·018
6	−0·035	0·013	0·054	0·155	0·352	0·336	0·174	0·123	0·004	−0·156	−0·041	−0·076
8	0·030	0·101	0·268	0·341	0·482	0·466	0·335	0·353	0·299	0·137	0·163	0·015
10	0·208	0·256	0·378	0·342	0·388	0·402	0·338	0·435	0·479	0·381	0·347	0·195
12	0·140	0·174	0·187	0·118	0·093	0·141	0·167	0·277	0·340	0·288	0·207	0·096
14	−0·142	−0·179	−0·226	−0·211	−0·237	−0·168	−0·054	−0·011	−0·008	−0·026	−0·121	−0·163
16	−0·290	−0·467	−0·581	−0·539	−0·546	−0·451	−0·281	−0·316	−0·345	−0·234	−0·284	−0·229
18	−0·252	−0·449	−0·539	−0·561	−0·663	−0·613	−0·416	−0·453	−0·407	−0·164	−0·221	−0·126
20	−0·138	−0·255	−0·187	−0·224	−0·439	−0·470	−0·298	−0·306	−0·187	0·030	−0·094	0·004
22	−0·011	−0·095	0·094	0·114	−0·090	−0·123	−0·006	−0·057	0·022	0·133	−0·011	0·126

balance S_f is still close to -1 regardless of phase. Likewise, C_{FD} connecting the dynamic series D_c and the magnitude of the acceleration F now has larger absolute values at phase -4^h and $+6^h$. However, C_{SD} is now almost zero which was to be expected.

It was hoped that the separation of the series $D(t)$ and $T(t)$ by means of the multicorrelation analysis would result in two corrected series with the property that a dataset, where the series $T_c(t)+D_c(t)$ had been subtracted from the observed series $O(t)$, would produce zero results in both of the programs used to compute $\overline{T}'(\nu)$ and $\overline{D}'(\nu)$. However, the tests showed that the resulting mean gradients were actually overcompensated, which was also the case in Part I where we had subtracted the original series $T(t)+D(t)$ (see Part I, p. 823). Therefore, the multicorrelation analysis seems to be a blind alley.

Statistical tests, however, revealed another result. If the program which determines the dynamic gradient $\overline{D}'(\nu)$ is run with the data $O(t)-D(t)$, the result becomes zero as expected. But if the same program is run with the data $O(t)-T(t)$, the result, perhaps surprisingly, is also zero. The series $T(t)$ with a period of 24 mean solar hours attains amplitudes about twice the amplitude of $D(t)$. To compensate the pressure oscillations following the more complicated pattern of tidal days, the explanation must be that an 'image' of $D(t)$ is contained in $T(t)$. The results of the tests are shown in Table 4, columns 2 and 3. We notice that the resulting gradients $\overline{D}'(\nu)$ are much smaller than the standard deviations in both cases.

A similar test on the program determining $\overline{T}'(\nu)$ with the data $O(t)-T(t)$ was of course expected to give a zero result, but if the series $T(t)$ really contains an image of $D(t)$ the test ought to be unaltered if we subtract the combination $T(t)-D(t)$ from the observed data $O(t)$. The results are shown in Table 4, columns 6 and 7. Comparison of the resulting gradients with the standard deviations demonstrates the validity of the assumption.

In order to be able to compare this with a dataset consisting of pure noise, two sets of artificial data were formed. The series $R(\frac{1}{2})$ and $R(1)$ consist of random numbers confined to the intervals $\pm\frac{1}{2}$ and ± 1 mb. In Table 4 column 4 the mean dynamic gradient with standard deviations is listed when the dataset $1013+R(\frac{1}{2})$ was used, and in column 8 the mean thermal gradient is shown with the data $1013+R(1)$. Consequently, the 'thermal' series $T(t)$ seems to contain an 'image' of the dynamic series of the same order of magnitude as $D(t)$ itself. This means that the 'true' thermal oscillation would be the series $T(t)-D(t)$.

In Table 5 we present the daily variation of the monthly means of the series (*a*) $T(t)$ and (*b*) $T(t)-D(t)$.

5. Conclusions

The results of the present investigation have been the detection of a one-day dynamic pressure oscillation with a mean amplitude of 0·17 mb, together with its first harmonic, a half-day oscillation with a mean amplitude of 0·048 mb. We may compare this with earlier results based on observations from the same station (Oslo) by Haurwitz and Cowley (1969), where only traces of a half-day oscillation with amplitude 0·007 mb were found.

Atmospheric tides ought to be re-investigated on a global scale.

References

Brahde, R. (1988). *Aust. J. Phys.* **41**, 807–31.
Chapman, S., and Lindzen, R. S. (1970). 'Atmospheric Tides' (Reidel: Dordrecht).
Haurwitz, B., and Cowley, A. D. (1969). *Pure Appl. Geophys.* **6**, 122–50.
Malin, S. R. C., and Chapman, S. (1970). *Geophys. J. R. Astron. Soc.* **19**, 15–35.

Manuscript received 1 February, accepted 26 April 1989